JOURNAL OF GEOPHYSICAL RESEARCH, VOL. 86, NO. C7, PAGES 6442–6450, JULY 20, 1981

Infragravity Energy in the Surf Zone

R. A. HOLMAN

School of Oceanography, Oregon State University, Corvallis, Oregon, 97331

Field measurements of onshore and longshore velocities in the surf zone have been obtained on Martinique Beach, Nova Scotia, for the purpose of investigating the dynamics of the infragravity band (0.003–0.03 Hz) of the spectra. A total of 35 data runs were obtained during a 1-week period. Of particular interest is the response of the infragravity energy to the changing incident waves, which increased considerably in size during the latter half of the week due to an approaching hurricane. It is shown theoretically, using equilibrium arguments, that the infragravity amplitude should vary approximately linearly with incident wave amplitude. This is supported from the field data if significant wave height is used as a measure of incident amplitude. The incident band of spectra observed by instruments in the surf zone is limited by breaking. Thus the infragravity band appears to dominate these spectra during storms. The analysis is carried out in terms of a spectral transformation, the spectrum which would be observed at an offshore instrument if the shoreline amplitude spectrum were white with unit spectral energy density. For onshore velocity the transformation predicts the observed spectral structure in the infragravity band, showing that the structure did not represent any true frequency selection. The match of theory and data also implies that the onshore motions are free waves, forced near resonance. The longshore spectra are red and show no structure which would be associated with free waves. This is consistent with the theoretical prediction that many edge wave modes, including high modes, would be forced given the broad directional spread of the storm waves. It is noted that further field experiments would be simpler on the Pacific coast where the typical, narrow-band, incident swell should force only a few, low, edge wave modes, a more accommodating situation to observe and analyze.

1. INTRODUCTION

The term 'infragravity' has been used to indicate motions with time scales of about 30–300 s, usually associated with the surf zone. *Munk* [1949] was the first to observe infragravity energy by using a tsunami recorder, basically a stilling well which filtered out the higher frequency components of the spectrum. He called the phenomenon 'surf beat' to reflect the observed association of these low frequency motions with the beat in the incident waves. The term infragravity energy is perhaps preferable to indicate that it is the low frequency motion that is being referred to, not the simple beating of two, first-order incident waves (which has no spectral representation at the beat frequency and does not necessarily provide the forcing at infragravity frequencies).

Theoretical studies of infragravity dynamics have evolved along two lines. The earlier theories were two dimensional, with no longshore dependence [*Munk*, 1949; *Tucker*, 1950; *Longuet-Higgins and Stewart*, 1964; *Suhayda*, 1974]. Associated with incident groups (defined by *Bowen* and *Guza* [1978] as the amplitude modulation in the incoming wave train) is a second-order, forced correction to mean sea level, progressing shoreward with the group. This forced wave is then released as a seaward-propagating free wave when the incident waves break [*Longuet-Higgins and Stewart*, 1964]. The summation of the inward and outward propagating components should give a standing component to the wave pattern. This mechanism does not allow for longshore periodicity, and the response is limited since the interaction is not resonant.

More recently, three -dimensional theories have been developed in which longshore modulation in the incident wave field is also considered. *Gallagher* [1971] was the first to discuss this case, showing that, under certain conditions, the incident wave groups could force edge waves. Longshore periodicity was thus introduced into the problem and, since the interaction could be resonant, the edge wave amplitude was not inherently limited. The mechanism was further discussed by *Bowen and Guza* [1978] who concluded from laboratory evidence that Gallagher's mechanism was important and that surf beat may in fact be primarily an edge wave phenomenon.

One important motivation for the study of the infragravity portion of the spectrum is to understand nearshore sediment transport and its role in the development of beach morphology. *Bowen and Inman* [1971] point out that the formation of crescentic sand bars can be explained in terms of standing, infragravity edge waves. Similarly, linear bars may be generated by progressive edge waves. However, for this to occur, the infragravity energy must be in the form of narrow spectral peaks which, for crescentic bars at least, should each contain only one edge wave mode.

Field investigations have found difficulty differentiating between standing incident and edge wave models for infragravity energy. This is largely due to the similarity in offshore profile of the two wave forms; an extensive instrument array would be needed to distinguish properly which wave form was present, particularly if many high edge wave modes were contributing to the wave motion. Thus past work has generally described infragravity spectra and shown consistency with one or the other theory. Data discussed in terms of the standing incident wave theory has been published by *Munk* [1949], *Tucker* [1950] and *Suhayda* [1974]. Field data which was explained in terms of edge waves was presnted by *Gallagher* [1971], *Huntley and Bowen* [1975], *Sasaki and Horikawa* [1975], and *Huntley* [1976].

Field studies have also attempted to test the relationship between infragravity waves and beach morphology [*Short*, 1975; *Wright et al.*, 1978]. Again, these studies were unable to identify the form of the infragravity energy. (It should be noted that this discussion purposely excludes the higher frequency subharmonic edge wave mechanism which *Guza and Inman* [1975] show can generate beach cusps. Greater success has been achieved in identifying subharmonic energy as edge

Paper 1C0314.
0148-0227/81/001C-0314$01.00

waves and linking these to beach features [*Komar*, 1973; *Huntley and Bowen*, 1978].)

Finally, several studies have demonstrated that beach morphology is most actively altered during storms [*Schalk*, 1963; *Short*, 1975]. It is therefore of interest to know if the infragravity band of the spectrum becomes increasingly important during storms. High energy conditions have been studied by *Wright et al.* [1978] and *Holman et al.* [1978].

The purpose of this paper is to study the nature of infragravity energy on a real beach and the variation of the infragravity response to varying incident wave energy. This is accomplished through the use of an extensive set of field data. The data are interpreted in terms of a superposition of edge wave modes. Section 2 therefore reviews some necessary theoretical ideas starting with basic edge wave kinematics. A spectral transformation, $M(f)$, is introduced as a necessary tool for the analysis of offshore data, and the method of application of the transformation to the data is discussed. Some general assumptions about the form of the forcing and damping terms on a natural beach are then used to extend the theory of edge wave dynamics. The physics described by the equations is then interpreted in terms of predicted edge wave mode selection and strength of the edge wave forcing. Conveniently, the form of the results is not sensitive to the precise forms of the assumptions. Finally, the response of the system under a variety of incident wave conditions is discussed. It is shown theoretically that only under very specific circumstances (a deep water angle of incidence nearly normal) would leaky modes be expected to dominate the infragravity band. Section 3 discusses the field observations of onshore velocity during storm conditions. In section 4 the field data from calm and storm runs are compared to determine the relationship between the incident energy and the infragravity response. Finally, section 5 discusses the field measurements of the longshore component of velocity.

2. THEORY

Edge Wave Kinematics

Edge waves are free surface gravity waves which propagate along a sloping beach, their energy trapped in the nearshore by refraction (there is no radiation to the far field). This permits amplitudes to be built up through weak incremental forcing. The edge wave solutions to the equations of motion have been found for several analytical expressions for the beach profile. The most commonly used is the shallow water solution of *Eckart* [1951] for a plane beach, $h(x, y) = x \tan \beta$, where x is the offshore coordinate, positive seaward from the still water shoreline, y is the longshore coordinate, h is the still water depth, and $\tan \beta$ is the beach slope. Eckart describes the edge waves in terms of the velocity potential, $\Phi(x, y, t)$, where the velocity, $\mathbf{u}$, and the elevation, η, are given by

$$\mathbf{u} = (u, v) = \nabla\Phi \qquad \eta = -\frac{1}{g}\frac{d\Phi}{dt} \tag{1}$$

where g is the gravitational acceleration and t is time. Eckart's solution consists of a set of edge wave modes, described by the integer modal number, n, and having the form

$$\Phi = \frac{a_n g}{\sigma} \cos(ky - \sigma t)\phi_n(x) \tag{2}$$

where a_n is the shoreline amplitude of the nth mode, σ is the radial frequency ($=2\pi/T$, where T is the edge wave period) and k is the wave number ($=2\pi/L$, where L is the longshore wavelength). The offshore behavior is expressed in terms of the nth order Laguere polynomial, L_n,

$$\phi_n(x) = e^{-kx} L_n(2kx) \tag{3}$$

The dispersion relation is

$$\sigma^2 = gk(2n + 1) \tan \beta \tag{4}$$

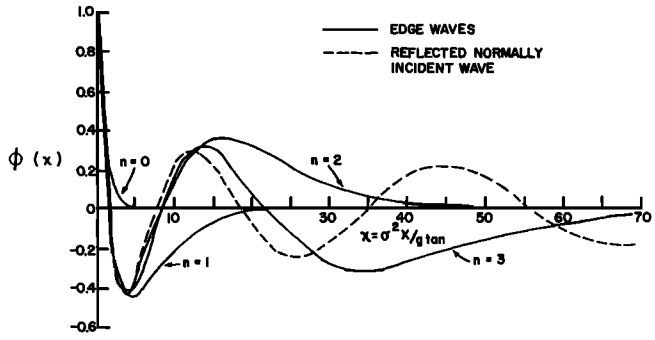

Fig. 1. Offshore dependence of edge waves of modes $n = 0, 1, 2, 3$ and of a reflected normally incident wave for a plane beach in terms of nondimensional offshore distance $x = \sigma^2 x/g\beta$.

Figure 1 is a plot of ϕ versus nondimensional offshore distance $\chi = \sigma^2 x/g\beta$ for edge wave modes 0 to 3. Also plotted is the offshore profile for a standing incident wave which is seen to be similar in form to the higher edge wave modes. For typical values of σ, x, and β for nearshore measurements of infragravity energy, χ is usually small, of the order of 5. For these values, the edge wave modes (with the exception of mode 0) and even the reflected, normally incident wave, are virtually indistinguishable.

As the offshore amplitude of an edge wave varies with x and σ, offshore data must be interpreted with this in mind. *Huntley* [1976] investigated the variation of energy in particular frequency bands with offshore distance, showing them to match well the predicted variation for edge waves (Figure 1). *Suhayda* [1974] carried out the analysis for a fixed offshore position, showing that the variability of energy with frequency was consistent with the modal structure for standing incident waves. The latter circumstance, with spectra measured at fixed offshore locations, is typical for field data. It is evident that all offshore data should be analyzed in terms of a spectral transformation, $M(x, f)$, to separate this expected spectral structure due solely to offshore position from that which represents real, physical processes. Suhayda carries this out assuming a plane beach. The assumption of a plane beach profile is often a good first approximation but plane beach profiles are not the norm in nature, concave profiles being more common [*Dean*, 1977]. An analytical solution for an exponential beach profile is provided by *Ball* [1967], but is difficult to use and of limited applicability since it assumes depth approaches an asymptotic value offshore. *Holman and Bowen* [1979] use a simple numerical scheme to solve the equations of motion for more realistic beach profiles, finding the dispersion relation and $\phi(x)$ for any edge wave frequency, σ.

Similarly the spectral transformation $M(f)$ must be found numerically. This is done for onshore velocity (for example) by numerically computing $u(x_i, f')$ for a set of values f', where u is calculated for unit shoreline amplitude and x_i is the instrument position. $M_u(f)$ is interpolated from the set of values

$M_u(x_i, f') = u^2(x_i, f')$. The transformation will be a function of instrument position and of tidal elevation since the latter affects the beach profile. M will also be mode dependent but only weakly so since the modes are so similar for typical χ values (Figure 1). Tests for Martinique Beach, Nova Scotia, showed $M_n(f)$ through the infragravity band to be virtually independent of mode for edge wave modes 2 or greater. Mode 4 was chosen for further calculations [*Holman and Bowen*, 1979].

The transformation is applied to the data by shifting the curve along the y axis to maximize the fit to the data. The amount of the shift is a measure of the shoreline energy (since the curve is calculated for unit shoreline amplitude) and can be used as a consistency check between instruments. Differences in the vertical shift between runs reflect time variations in the infragravity energy. Differences between the data and the shifted transformation in a particular run represent true structure in the shoreline amplitude spectrum.

Edge Wave Dynamics

Infragravity waves are most likely forced through a nonlinear interaction within a modulated incident wave field. The formalism for this interaction has been discussed by *Gallagher* [1971], *Witham* [1976], and *Bowen and Guza* [1978]. In general terms, the surface boundary condition for the problem is expressed, to second order, as

$$L(\Phi_2) = Q(\Phi_1, \Phi_1) \tag{5}$$

Q is a quadratic operator describing the interaction of two first-order waves, in this case taken to be two incident waves. The interaction will force Φ_2, a motion which must satisfy (5). The nonlinear forcing, $Q(\Phi_1, \Phi_1)$, will occur at frequency

$$\sigma_f = |\sigma_1 - \sigma_2| \tag{6a}$$

and the longshore component of wave number will be

$$k_f = k_{y_1} - k_{y_2} = k_1 \sin \alpha_1 - k_2 \sin \alpha_2 \tag{6b}$$

where the subscripts 1 and 2 refer to the two, interacting, incident waves, and α is the angle of incidence. *Ursell* [1952] shows that the complete set of solutions, Φ_2, on a beach consists of the set of discrete edge wave modes, for which $\sigma^2 < gk_y$, and a continuum of leaky modes, for which $\sigma^2 > gk_y$ (Figure 2).

The interaction of the incident groupiness and a particular edge wave mode will be resonant if σ_f and k_f satisfy the edge wave dispersion relation. *Bowen and Guza* [1978] discuss this case, showing that the edge wave amplitude, a_e, will grow as

$$\frac{\partial a_e}{\partial t} \sim \frac{a_1 a_2}{2g} \frac{\int_0^\infty f(x)\phi_n(x)\,dx}{\int_0^\infty \phi^2(x)\,dx} \tag{7}$$

where a_1 and a_2 are the amplitudes of the incident waves and $f(x)$ is a complicated expression describing the offshore shape of the incident wave forcing pattern arising from the beating. The integral in the numerator describes the coupling of the forcing pattern and the edge wave. The integral in the denominator is the necessary normalization. (In practice, the breaking process reduces the incident groupiness in the surf zone, and it is convenient to ignore this region, starting the integral at the mean break point. This leads to an incident amplitude dependence somewhat less than quadratic.)

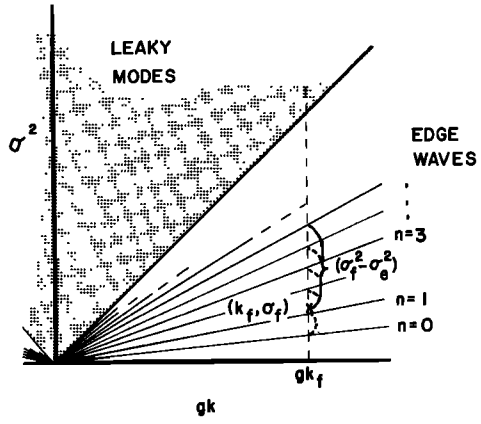

Fig. 2. The complete set of solutions Φ_2, consisting of the edge wave regime and the leaky mode regime. Incident forcing at (k_f, σ_f) will force all edge wave modes with wave number k_f. The strength of the forcing depends on $\sigma_f^2 - \sigma_e^2$ (equation (10)).

Although the details of the calculation can be complicated, one important conclusion can be drawn. Regardless of the details of $\phi(x)$ and $f(x)$, both factors are known to increase toward the shoreline. Thus the dominant contribution to the coupling integral (7) will be in the nearshore (generally $\chi \leq 10$ for examples calculated numerically) with offshore contributions being negligible. The similarity of the offshore profiles of the different edge wave modes in this region has already been pointed out. Thus we expect that the coupling integral will be only weakly mode dependent. (In fact, k, which is mode dependent, enters the integral, but numerical examples have shown the dependence to be very weak.)

In the absence of a significant longshore current, edge wave dissipation will depend on the relative importance of $\mathbf{u}_e$, a typical edge wave velocity, and u_{orb}, a typical incident wave orbital velocity. For $|\mathbf{u}_e| \ll u_{orb}$ an approach may be used similar to that used by *Longuet-Higgins* [1972] in modeling dissipation of a steady longshore current in the presence of breaking waves; that is, friction term $= (C/h)u_{orb}\mathbf{u}_e$, where C is the drag coefficient. This gives rise to friction damping of the form:

$$\frac{\partial a_e}{\partial t} \sim -a_e a_i \frac{\int_0^\infty f'(x)\phi_n(x)\,dx}{\int_0^\infty \phi_n^2(x)\,dx} \tag{8}$$

where $f'(x)$ describes the offshore dependence on the product of incident wave amplitude, a_i, and the edge wave amplitude, a_e.

Equation (8) is only a crude representation of dissipation. *Guza and Bowen* [1976], found that edge wave damping was dominated by surf zone turbulence when the incident waves break. In that case the offshore limit of the damping integral in (8) may be replaced by the break point, which depends on a_i, so the dependence of dissipation on a_i may be stronger than linear. On the other hand, the assumption $|u_e| \ll u_{orb}$ is sometimes locally violated in the inner surf zone (Figures 6 and 7), although contributions from this region to the offshore integral may not be large. Nevertheless, there may be some argument for the use of the friction term $(C/h)|\mathbf{u}_e|u_e$. Interestingly, the results derived in the following paragraphs are not sensitive to this change. The only difference will be in the

details of the integral; the predicted dependence of a_e on a_i will be unaffected.

For equilibrium, neglecting higher-order interactions, forcing equals dissipation. Comparing (7) and (8) suggests that the equilibrium edge wave amplitude may vary as

$$a_e \sim a_i \frac{\int_0^\infty f(x)\,\phi n(x)\,dx}{\int_0^\infty f'(n)\,\phi n(x)\,dx} \tag{9}$$

Equation (9) suggests that the relative importance of the infragravity and incident bands will be approximately independent of incident amplitude. Both integrals in (9) are dominated by conditions very close to the shore, which, for typical infragravity frequencies, corresponds to small χ. Thus, for the case of two, deterministic, incident waves, the resulting equilibrium edge wave amplitude will have at most a weak mode dependence. This result is general, being insensitive to the details of the forcing or damping models.

Typically, the forcing will not be exactly resonant. A forced edge wave response will be at the wave number and frequency of the forcing, (k_f, σ_f), and will vary as

$$a_e \propto \left[(\sigma_f^2 - \sigma_e^2)^2 + \frac{\sigma_f^2\sigma_e^2}{Q^2}\right]^{-1/2} \tag{10}$$

Q is the quality factor, an inverse measure of damping, and σ_e is the natural frequency of the edge wave [*Garrett*, 1972].

Figure 2 shows the complete set of second-order waves, Φ_2, and an example of forcing at (k_f, σ_f) which lies in the edge wave domain but between modes. For strong damping the edge wave response will be broadbanded, and many edge wave modes may be forced at σ_f. In most cases this forcing frequency will not correspond to that for a free edge wave. Thus spectra of measurements at fixed instruments will not show any particular structure as described by the spectral transformation. On the other hand, the observation of such structure in field spectra implies that only near-resonant modes ($\sigma_e \sim \sigma_f$) contribute significantly. This is only true if the damping is weak (large Q) and the resonances are sharp.

If the forcing lies in the leaky mode regime, $\sigma_f^2 > gk_f$, the offshore motion is described by the confluent hypergeometric function [*Guza and Davis*, 1974]. *Guza and Bowen* [1976] show that for typical field values of beach slope and deep-water angle of incidence, this offshore behavior can be closely approximated by the zeroth order Bessel function, J_0 $[(4\sigma^2 x/g\beta)^{1/2}]$ [see also *Suhayda*, 1974]. Figure 1 shows J_0 to be virtually indistinguishable from most edge wave modes for small χ. All edge modes with wave number k_f will also be forced, their response bring described by (10). The observation of spectral structure as described by $M(f)$ again implies that near-resonant modes dominate.

Bowen and Guza [1978] describe the distribution of k_f, σ_f under natural stochastic forcing. If the incident spectrum is restricted in direction to a beam of central angle of incidence α and beamwidth $\Delta\alpha$, then the possible pairs of incident angles, α_1, α_2, will be shown be a conceptual interaction circle (Figure 3). Each point in the circle represents a particular incident forcing, k_f, σ_f, which can be determined from (6) (given σ_1 and σ_e). A free edge wave mode will be resonantly forced if

$$\sin\alpha_1 = [1 - (\sigma_e/\sigma_1)]^2 \sin\alpha_2 \pm \frac{1}{\sin(2n+1)\beta}(\sigma_e/\sigma_1)^2 \tag{11}$$

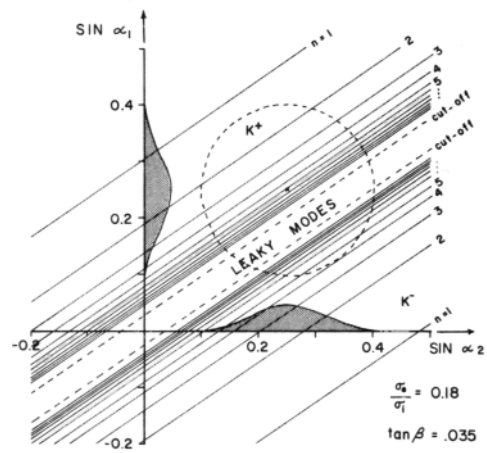

Fig. 3. Example of the resonant conditions for excitation of an edge wave with frequency σ_e, mode number n, by two incident waves with frequencies σ_1, σ_2, on a beach of constant slope β. The shaded area indicates the distribution of direction of incidence $\alpha = 15° \pm 10°$. The dashed circle then indicates the zone of incident wave forcing. Forcing exists in the edge wave and leaky mode regimes although the most likely interaction (the center of the interaction circle) lies in the edge wave regime [after *Bowen and Guza*, 1978].

These resonances are shown, for various n, in Figure 3 by the straight lines. Also shown is the leaky mode regime. It is clear that, for this example, many edge wave modes will be resonantly forced as well as the leaky modes. In fact, this will always be true for beamwidths of this order ($\Delta\alpha = 10°$). For very narrow beamwidths (of the order of 1° or less), Bowen and Guza's analysis of the colinear limit suggests that the forcing will be the strongest in (the interaction circle will be centered in) an edge wave regime out to a frequency

$$\sigma_f = 2\bar{\sigma}_i \sin\alpha \tag{12}$$

where $\bar{\sigma}_i$ is the mean incident frequency. Thus, only for the case of near-normal incidence and very narrow beamwidth will the forcing at very low frequencies not be strongest in an edge wave regime.

A connection can thus be made between the observation of spectral valleys at predicted modal frequencies and the conclusion that free edge waves dominate the flow. The train of reasoning is as follows. The observation of spectral valleys at proper frequencies implies that off-resonance forcing is comparatively small. This is true only for high Q (weakly damped) systems. Our understanding of nonlinear forcing for a realistic incident wave field indicates the extreme likelihood of resonantly forcing many edge wave modes as well as leaky modes and, in fact, the likelihood that the strongest forcing will be in the edge wave regime for low frequencies. Finally, for a high Q system, resonantly forced edge waves, whose energy remains trapped to the nearshore, should dominate over leaky modes whose energy is continually radiated away to the far field. Thus the initial observation of the spectral valleys is a strong indication that free edge waves should dominate the motion.

3. FIELD OBSERVATIONS

A field program to study the infragravity band of the spectrum was carried out on Martinique Beach, Nova Scotia, in August 1976. A total of 35 data runs were taken over a 1-week period. The run length was chosen as 50 min, the maximum

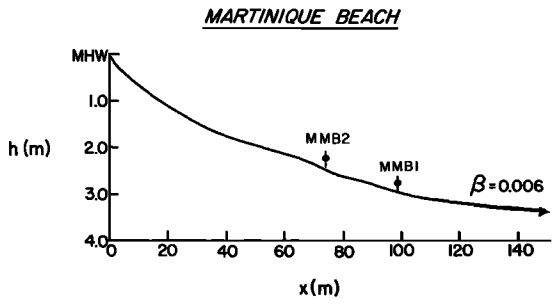

Fig. 4. Profile for Martinique Beach and location of flowmeters.

felt possible without losing stationarity in the face of a changing tide, the mean tidal range being 1.5 m. The runs were centered at high, low, and middle tides, although some early runs were missed due to equipment problems.

The data were collected by using three electromagnetic flowmeters. The results of two of these, deployed on an offshore transect, will be discussed in this paper. The positions of the two ball-type flowmeters (labeled MMB1 and MMB2 because they are of Marsh-McBirney manufacture) and the measured beach profile are shown in Figure 4. Sonar data, taken in 1974, showed the offshore profile to be almost plane out to 2 km with a slope of 0.006, shown patched to the nearshore profile in Figure 4.

The data set is of particular interest because extremes of incident conditions were experienced through the week. The first half of the week, corresponding to runs 1–20, was calm with only low-amplitude, long-crested swell. Storm conditions prevailed for the second half of the week (runs 21–35), a result of the close passage of hurricane Belle [*Holman et al.*, 1978]. These sharply changing incident conditions provide an excellent opportunity to investigate the response of the infragravity band. Further details of the experiment and some initial analysis and interpretation are contained in *Holman et al.* [1978]. The more extensive analysis described below modifies some of our original interpretations.

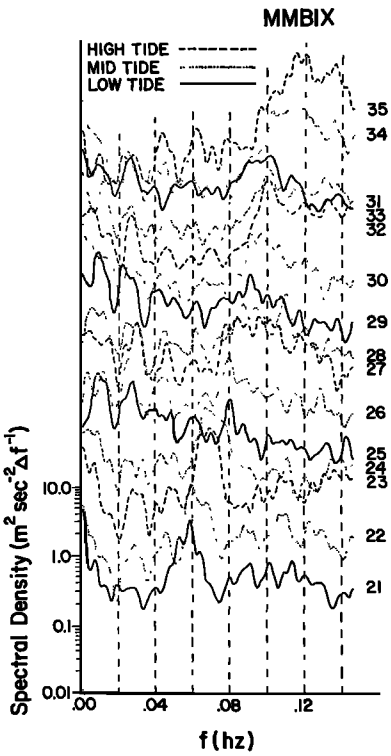

Fig. 5*a*. Spectral time series of onshore velocity for MMB1 during storm conditions.

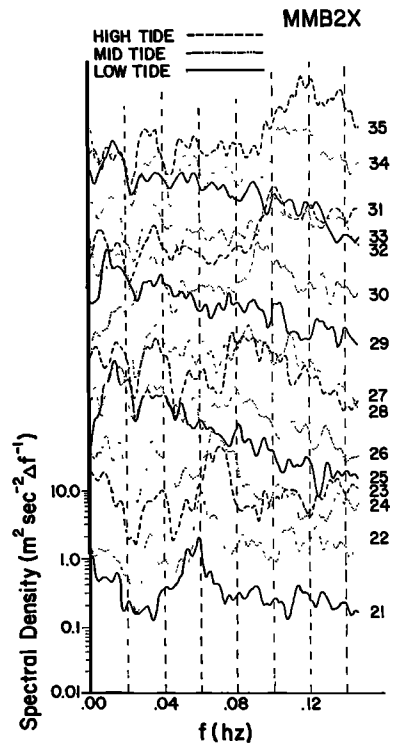

Fig. 5*b*. Spectral time series of onshore velocity for MMB2 during storm conditions.

Figures 5*a* and 5*b* show spectral time series of onshore velocity for the two instruments during the storm conditions. A spectral time series is just a sequence of individual spectra with each spectrum offset slightly from the previous to give a visual impression of how the energy in each frequency band varies with time. In this case the offset is vertical to allow simple comparison of the frequencies of different features. Here, 95% confidence limits are 0.6 and 1.9 times the spectral estimate (24 degrees of freedom). The bandwidth for the 10-point Tukey filter is 0.0044 Hz. Data from all stages of the tide are shown. Examination of run 21 in Figure 5 shows an energetic swell peak at 16 s (0.0625 Hz), which *Holman et al.* [1978] identified as the storm forerunners. In subsequent runs this peak shifts to higher frequencies as the storm approaches, in agreement with the known dispersion of storm-generated waves [*Munk et al.*, 1963]. The overall impression of the infragravity band is that there is considerable structure present.

Analysis was carried out in terms of the spectral transformation for onshore velocity, $M_u(f)$. Figures 6*a*, 6*b*, 6*c*, and 6*d* show storm spectra from a high and low tide run (runs 23 and 25, respectively) for each of the two instruments. Superimposed over the infragravity band is the spectral transformation, $M_u(f)$, for each case. The energy scale for $M_u(f)$ is three decade logarithmic, the same as the data, but the transformation has been shifted along the y axis to maximize the fit.

The similarity of the data and transformations in Figure 6 is striking. Most obvious is the ability of the transformation to explain the spectral valleys, the main features of the spectra. Interestingly, M_u correctly predicts the shift of the valleys with tide, showing that a rise in tide is accompanied by a shift of

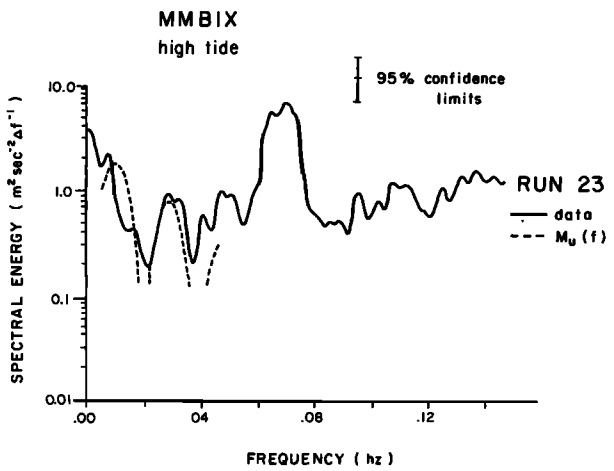

Fig. 6a. Comparison of a high tide storm spectrum with the spectral transformation, $M_u(f)$, for MMB1.

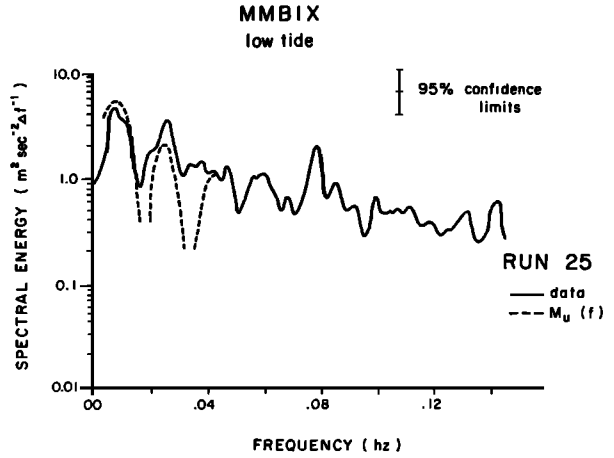

Fig. 6c. Comparison of a low tide storm spectrum with $M_u(f)$ for MMB1.

the first spectral valley to higher frequencies for MMB1 but to lower frequencies for MMB2. The possibility of this behavior, contrary to intuition based on plane beach theory, was pointed out by *Holman and Bowen* [1979] as resulting from beach concavity.

As was pointed out in the theory section, the similarity of the spectral transformation and the data in the infragravity band is strong evidence that the flow was dominated by free edge wave modes.

Comparison of the apparent infragravity peaks with those predicted by the transformation shows some differences but, in general, good agreement. What differences do exist are consistent between instruments for a particular stage of tide, an encouraging check of the model, and evidence that the differences represent real structure in the equivalent shoreline spectrum. For the low tide spectra, the transformation overpredicts the energy of the first peak but underpredicts that of the second. This implies that the true shoreline amplitude spectrum was not white, but was blue, showing energy increasing with frequency. The high tide data is somewhat obscured by the presence of a spectral redness at very low frequencies. The nature of this energy is not known, but *Holman* [1979] suggests, based on cross-spectral analysis, that it may be in the form of forced oscillations, not free waves. Excluding this very low frequency energy, the transformation overpredicts the first spectral peak but matches well the second peak. This again indicates a blue trend to the equivalent shoreline amplitude spectrum, although possibly not as strong as it was for the low tide case.

The degree of shift of the transformation curves were measured. The measured values correspond to an equivalent shoreline energy level of 1.8 $m^2 \Delta f^{-1}$ (the curve, $M_u(f)$, calculated for unit shoreline energy level, had to be shifted up slightly) for low tide and 1.2 $m^2 \Delta f^{-1}$ for high tide. This increased energy at low tide is contrary to the speculation of *Holman and Bowen* [1979] and is not understood.

It should be noted that if the infragravity energy is, in fact, in the form of edge waves, then to explain the presence of two (or three) spectral valleys requires that a significant proportion of the energy be in modes 2 (or 3) or greater.

4. Infragravity Response to High and Low Energy Incident Forcing

Figures 7a and 7b compare onshore velocity spectra for MMB2 for storm and calm conditions. Runs 12 and 25 are typical low tide examples of low and high energy respectively, while runs 13 and 27 are typical for high tide. It is immediately evident that the increase in infragravity band energy is much stronger than the linear dependence on incident energy suggested by the theory. However, it must be remembered

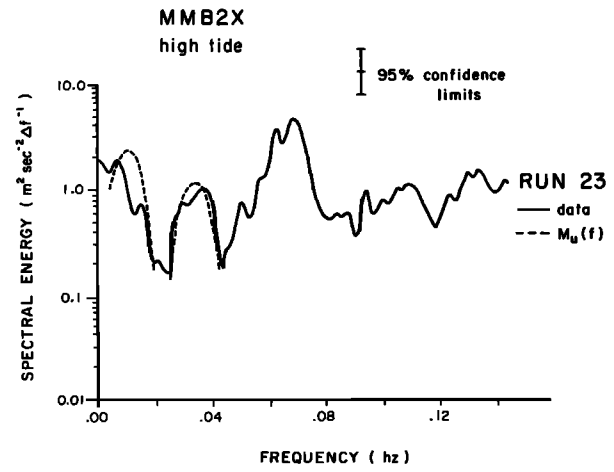

Fig. 6b. Same as Figure 6a but for MMB2.

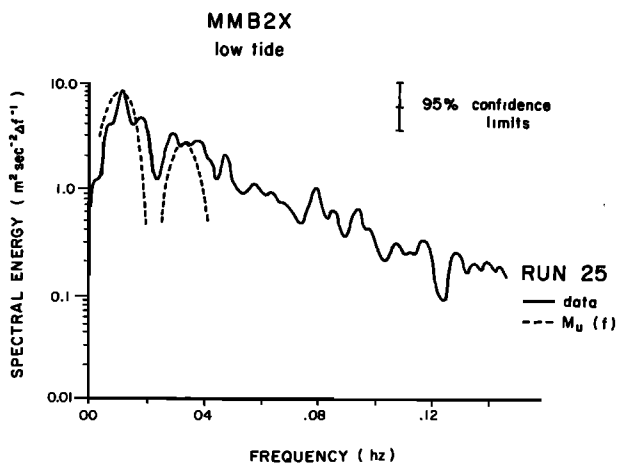

Fig. 6d. Same as Figure 6c but for MMB2.

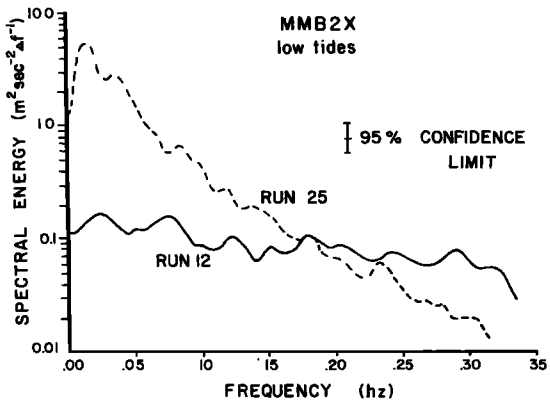

Fig. 7*a*. Comparison of a typical low energy (solid line) and high energy (dashed line) onshore velocity spectrum for MMB2 during low tides.

that the data presented in Figure 7 are from within the surf zone where the increase in incident energy observed by an instrument is limited by the breaking process.

A more appropriate test of the theory would require observations from an instrument placed outside the surf zone. In the absence of such data, the visually observed significant wave height may be used as a rough measure of a_i. Taking U to be the orbital velocity which represents the energy in the infragravity band,

$$U = \left[2 \int_{0.00}^{0.05} S_{uu}(f)\, df \right]^{1/2}$$

where S_{uu} is the spectral energy density, and f is the frequency in hertz, then Figure 8 shows the dependence of U on the significant wave height $H_{1/3}$. While some scatter exists, the trend can reasonably be approximated as linear, in support of the theoretical prediction.

While the data presented in Figure 7 are inappropriate to test the theoretical amplitude dependence of a_e on a_i, they are appropriate to the understanding of sediment transport processes in the surf zone. The sediment will respond only to the local fluid motion. The observation of the increased relative importance of the infragravity band during storms suggests that sediment transport processes in the surf zone will be increasing dominated by the infragravity band during high energy conditions.

5. LONGSHORE VELOCITY SPECTRA

Figure 9 shows a spectral time series for the longshore velocity component for MMB2 during storm conditions. A very low frequency spectral redness is present in all runs, similar to that noted in Figure 6*a*. Again cross-spectral analysis shows low coherence between instruments for the very low frequencies, possibly indicating a forced motion. Some structure exists in the infragravity band but, contrary to the onshore velocity spectra, neither peaks nor valleys are consistent run to run. This implies that the longshore energy is predominantly in the form of forced oscillations without the frequency-length scale relationship shown in the onshore spectra. The observation of wave-associated motions in the onshore velocity spectra only is consistent with an edge wave explanation only if a number of higher edge wave modes contribute. This is because the longshore component of velocity becomes decreasingly important with increasing edge wave modal number. For edge waves on a plane beach the ratio of longshore to onshore velocity at the shoreline falls off very rapidly with mode

$$\frac{v(x=0)}{u(x=0)} = \frac{1}{2n+1}$$

For offshore positions and for concave beach profiles the modal number dependence is reduced, but it is clear that the inclusion of significant energy contributions from higher modes will reduce the relative importance of the longshore velocity, possibly allowing it to be dominated by forced oscillations.

The ideas advanced in the theory section showed that the strength of the forcing and damping were not significantly mode dependent, nor were the resonant restrictions imposed by restricting incident wave direction to a beam, provided the incident beam width was moderately large. For this data set the incident beam width is assumed to have not been small, although it was not measured. Support for the assumption comes from the low u, v coherences observed in the incident band for each instrument. *Battjes* [1972] demonstrates the reduction in the S_{xy} value of radiation stress (and similarly the u, v coherence) caused by allowing a spread in angle of incidence. The observed coherences of less than 0.3 correspond to a very weak directional dependence. Visual observations also confirmed the short crestedness in the incident wave field. Thus we do expect to see many high modes contributing to the spectrum. The lack of structure, predicted by the spectral transformation, in the longshore velocity spectra is then consistent with an edge wave explanation.

It may quickly be pointed out that the observed data are consistent with a standing incident wave explanation and that this data set, like others in the past, is unable to definitively distinguish between the two mechanisms. However the theory presented in this paper (which is relatively general) suggests that, as long as the incident beam width is moderately large, this distinction may never be made; a large number of high modes will always be forced, and the resulting motion will be complex. This will be the typical case for Atlantic beaches. We would be better able to make the distinction on the Pacific coast where narrow beam widths typify the long Pacific swell. *Bowen and Guza* [1978] predict only a few low modes would be forced in that case giving a much simpler sampling problem and much greater chance of successfully distinguishing individual edge wave modes.

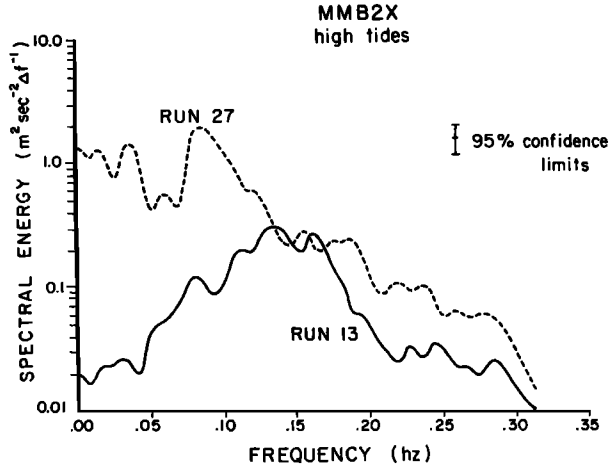

Fig. 7*b*. Same as Figure 6*a* but for high tides.

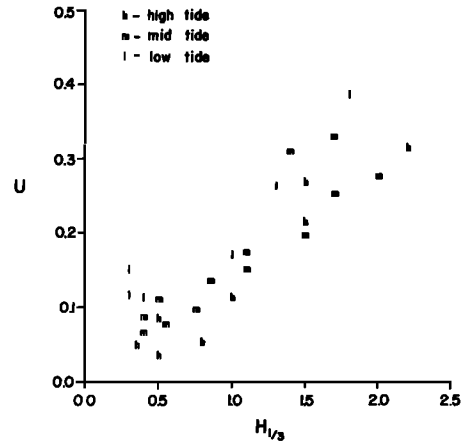

Fig. 8. Variation of U, an orbital velocity which represents the energy in the infragravity band, with visually observed significant wave height for high, middle, and low tide.

CONCLUSIONS

Field data of onshore velocity taken by flowmeters at fixed positions within the surf zone showed significant spectral structure through the infragravity band. However, analysis of the spectra by using a spectral transformation (generating the spectrum that would be seen at a particular offshore location for a white shoreline amplitude spectrum unit energy density) showed that most of the structure was due to instrument position and did not represent frequency selection. The equivalent shoreline amplitude spectrum was slightly blue with a mean energy density of 1.2 m^2 s at high tide and 1.8 m^2 s at low tide. The observation of spectral valleys in the data at frequencies predicted by the spectral transformation suggests that the wave motions are forced only near resonance (i.e., the system has a relatively high Q). The observation of two spectral valleys in each offshore velocity spectrum implies the wave motion has at least two offshore zero crossings. If the wave motion were in the form of edge waves, then significant energy must have been present in modes two or greater.

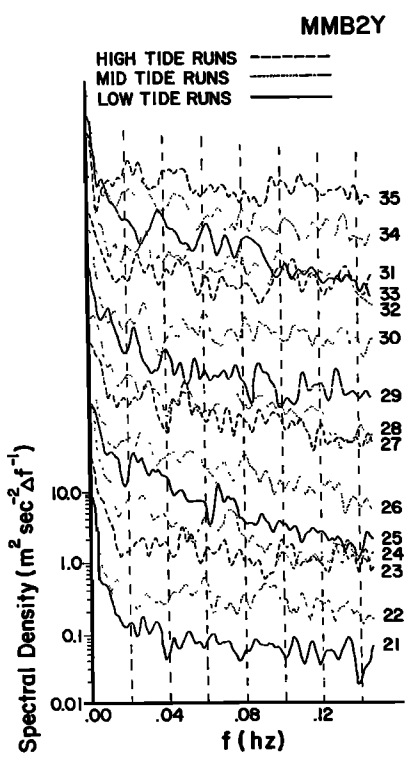

Fig. 9. Spectral time series of longshore velocity for MMB2 during storm conditions.

Longshore spectra do not show the equivalent, wave-associated, spectral features, indicating a dominance of motions forced off resonance. This is consistent with an edge wave model provided high edge wave modes contribute a significant portion of the energy. *Bowen and Guza* [1978] study the effect of the resonant conditions (4, 6) on the ability of an incident spectrum to resonantly excite edge waves of various modes. For the relatively broad directional spread of the storm waves suggested by the low u, v coherences in the incident band and the visual observations for this data set, *Bowen and Guza* [1978] predict that many edge wave modes, including all the high modes should be resonantly forced although the strength of the forcing will depend on the dynamics and may be a function of the particular mode.

By using general assumptions about the form of the nonlinear forcing and the damping, an equilibrium edge wave amplitude, a_e, can be predicted. The terms in the algebraic expression all grow toward the shoreline indicating that the integrals involved in the calculation of a_e will be dominated by the nearshore region. The similarity of the offshore structure of most edge wave modes in the nearshore then suggests that the dynamics of the edge wave forcing will be, at most, weakly mode dependent.

The theoretical equation for the equilibrium edge amplitude predicts that a_e should vary in an approximately linear fashion with the incident amplitude a_i. Comparison of the variations of U, an orbital velocity which represents the infragravity band energy, with the visually observed significant wave height is in very good agreement with this predicted linear dependence. Velocity spectra taken from within the surf zone can show only a limited increase in incident wave energy; breaking limits the wave height to a simple proportion of depth. No such limit exists for infragravity waves. Thus the observed spectra show increasing dominance by the infragravity band during storms. This is an important result for beach morphology, indicating that sediment transport in the surf zone may be dominated by low frequency motions during storms.

For the moderate directional spreads which typify Atlantic coast incident spectra, the interaction conditions suggest that many edge wave modes will be resonantly forced. The resulting wave motion will be the sum of the contributions from each mode and may be quite complicated to analyze. A much simpler motion may occur on the Pacific coast where narrow beamwidths typify the long ocean swell. In that case only a few low edge wave modes should be forced, giving a much simpler sampling problem and a greater chance of successfully distinguishing individual edge wave modes.

REFERENCES

Ball, F. K., Edge waves in an ocean of finite depth, *Deep Sea Res., 14,* 79–88, 1967.

Battjes, J. A., Radiation stresses in shore-crested waves, *J. Mar. Res., 30,* 56–64, 1972.

Bowen, A. J., and R. T. Guza, Edge waves and surf beat, *J. Geophys. Res., 83,* 1913–1920, 1978.

Bowen, A. J., and D. L. Inman, Edge waves and crescentic bars, *J. Geophys. Res., 76,* 8662–8671, 1971.

Dean, R. G., Equilibrium beach profiles: U.S. Atlantic and Gulf coasts, *Ocean Eng. Rep. 12,* Dep. of Civil Eng., Univ. of Delaware, Newark, 1977.

Eckart, C., Surface waves on water of variable depth, *Wave Rep. 100,* Scripps Inst. of Oceanogr., Univ. of Calif., La Jolla, 1951.

Gallagher, B., Generation of surf beat by non-linear wave interaction, *J. Fluid Mech., 49,* 1–20, 1971.

Garrett, C. J. R., Tidal resonances in the Bay of Fundy and Gulf of Maine, *Nature, 238,* 441–443, 1972.

Guza, R. T., and A. J. Bowen, Resonant interactions for waves breaking on a beach, *Proc. Conf. Coastal Eng. 15th,* 560–579, 1976.

Guza, R. T., and R. E. Davis, Excitation of edge waves by waves incident on a beach, *J. Geophys. Res., 79,* 1285–1291, 1974.

Guza, R. T., and D. L. Inman, Edge waves and beach cusps, *J. Geophys. Res., 80,* 2997–3012, 1975.

Holman, R. A., Infragravity waves on beaches, Ph.D. thesis, Dalhousie Univ., Halifax, 1979.

Holman, R. A., and A. J. Bowen, Edge waves on complex beach profiles, *J. Geophys. Res., 84,* 6339–6346, 1979.

Holman, R. A., D. A. Huntley, and A. J. Bowen, Infragravity waves in storm conditions, *Proc. Conf. Coastal Eng. 16th,* 268–284, 1978.

Huntley, D. A., Long-period waves on natural beaches, *J. Geophys. Res., 81,* 6441–6449, 1976.

Huntley, D. A., and A. J. Bowen, Field observations of edge waves and their effect on beach material, *J. Geol. Soc., 131,* 68–81, 1975.

Huntley, D. A., and A. J. Bowen, Beach cusps and edge waves, *Proc. Conf. Coastal Eng. 16th,* 1378–1393, 1978.

Komar, P. D., Observations of beach cusps at Mono Lake, California, *Geol. Soc. Am. Bull., 84,* 3593–3600, 1973.

Lamb, H., *Hydrodynamics,* 6th ed., Dover, New York, 1932.

Longuet-Higgins, M. S., Recent progress in the study of longshore currents, in *Waves on Beaches,* edited by R. E. Meyer, Academic, New York, 1972.

Longuet-Higgins, M. S., and R. W. Stewart, Radiation stresses in water waves: A physical discussion, with applications, *Deep Sea Res., 11,* 529–562, 1964.

Munk, W. H., Surf beats, *Eos Trans. AGU, 30,* 849–854, 1949.

Munk, W. H., G. R. Miller, F. E. Snodgrass, and N. F. Barber, Directional recording of swell from distant storms, *Phil. Trans. R. Soc. London, Ser. A, 255,* 505–584, 1963.

Sasaki, T., and K. Horikawa, Nearshore current system on gently sloping bottom, *Coastal Eng. Japan, 18,* 123–142, 1975.

Schalk, M., Study of nearshore bottom profiles east and southwest of Point Barrow, Alaska: Comparison of profiles and the barrier islands in the Point Bay and Plover Island areas, final report, Arctic Inst. North America, Washington, D. C., 1963.

Short, A. D., Multiple offshore bars and standing waves, *J. Geophys. Res., 80,* 3838–3840, 1975.

Suhayda, J. N., Standing waves on beaches, *J. Geophys. Res., 72,* 3065–3071, 1974.

Tucker, M. J., Surf beats: Sea waves of 1 to 5 minutes period, *Proc. R. Soc. A, 202,* 565–573, 1950.

Ursell, F., Edge waves on a sloping beach, *Proc. Roy. Soc. A, 214,* 79–97, 1952.

Witham, G. B., Non-linear effects in edge waves, *J. Fluid Mech., 74,* 353–368, 1976.

Wright, L. D., B. G. Thom, and J. Chappell, Morphological variability of high energy beaches, *Proc. Conf. Coastal Eng. 16th,* 1180–1194, 1978.

(Received February 1, 1980;
revised January 6, 1981;
accepted February 23, 1981.)